Mediterranean Archaeology and Archaeometry, Vol. 17, No. 1 (2017), pp. 47-68

DOI: 10.5281/zenodo.258085

INVESTIGATING THE PROVENANCE OF THE BAETICAN AMPHORAE DRESSEL 23: NEW ARCHAEOMETRIC EVIDENCE FROM LATE ROMAN CONSUMPTION CENTRES

L. Fantuzzi[1], M.A. Cau[*,1,2,3]

[1] Equip de Recerca Arqueològica i Arqueomètrica de la Universitat de Barcelona (ERAAUB), Departament d'Història i Arqueologia, Facultat de Geografia i Història, Universitat de Barcelona, c/ Montalegre 6-8, 08001 Barcelona, Spain
[2] ICREA, Pg. Lluís Companys 23, 08010 Barcelona, Spain
[3] Joukowsky Institute for Archaeology and the Ancient World, Brown University, Box 1837/60 George Street, Providence, RI 02912, USA

Received: 06/08/2016
Accepted: 23/12/2016
**Corresponding author: Miguel A. Cau (macau@ub.edu)*

ABSTRACT

Baetican amphorae of the type Dressel 23 found in Late Roman consumption centres from the northeastern Iberian Peninsula and the Balearic Islands were archaeometrically investigated in order to characterise the materials and examine their provenance. A combination of analytical techniques was used, including optical microscopy (thin-section analysis), X-ray fluorescence, X-ray diffraction and scanning electron microscopy. The results show two main fabrics and a number of other less represented fabrics. Some of these fabrics comprise all the samples of the variants Dressel 23a and 23c, and can be related to a provenance in the Guadalquivir/Genil valleys, while other fabrics include all the Dressel 23d samples and their provenance must be situated in the coastal area of Málaga, based on their petrographic composition and the integration of the archaeological information. Some samples of Almagro 51A-B amphorae are also analysed, and show the same chemical-petrographic composition as the Dressel 23d individuals, this indicating that they both come from the same workshops. The results suggest that the arrival of Dressel 23 amphorae from the Málaga area to the analysed consumption centres may have been more significant in the Late Roman period than usually acknowledged.

KEYWORDS: amphora, Hispania, Late Antiquity, provenance, petrography, XRF, XRD, SEM

1. INTRODUCTION

During the Late Roman period, a large-scale trade of foodstuffs transported in amphorae took place across the Mediterranean. The south of the Iberian Peninsula was one of the main production areas (see for example: Alarção and Mayet, 1990; Mayet *et al*., 1996; Bernal, 2001; Bernal and Lagóstena, 2004; Fabião, 2008; García Vargas and Bernal, 2008). A large amount and variety of Baetican and Lusitanian amphorae have been documented in many consumption centres, especially in the western Mediterranean, including, among others, the current Catalan area (*e.g*. Keay, 1984; Járrega, 1993, 2013; Berni, 1998; Remolà, 2000; Cela and Revilla, 2004; Reynolds, 2010).

One of the main southern Hispanic amphora types for this period is Dressel 23, with a wide chronology from the late 3rd century to the first quarter or first half of the 6th century. This type, also known as Keay 13, mainly used for olive oil from the Guadalquivir and Genil valleys (between *Corduba*/Córdoba and *Hispalis*/Sevilla), where about twenty workshops are mentioned by Remesal (1983, 1991), all of them with a continuous activity from the Imperial period. Clear archaeological evidence of the production of Dressel 23 is available for only a few of these workshops (Figure 1) (Remesal, 1983, 2004; Berni, 1998; Romo and Vargas, 2001; Chic and García Vargas, 2004; Berni and Moros, 2012a, 2012b). The best known of these is El Tejarillo, excavated in 1981 (Remesal, 1983). In these workshops, other types apart from Dressel 23 are more rare, including Tejarillo I (mid 3rd century to early 4th century) and the poorly known types Tejarillo III and Almagro 55/Keay 15 (Remesal, 1983; Berni, 1998).

Other workshops that produced Dressel 23 amphorae have been located on the Málaga coast (Figure 1) (Baldomero *et al*., 1997; Bernal, 1997, 2001; Rodríguez, 1997; Serrano, 2004; García Vargas and Bernal, 2008; Corrales *et al*., 2011). In this case, the workshops are associated with a significant production of other Late Roman amphora types, especially Almagro 51A-B (in particular the variant Keay 19A-B) and Almagro 51C/Keay 23, both related to the transport of fish sauces (Bernal, 2001). Also on the coast of Granada, there is evidence of a possible minor production of Dressel 20 or 23 amphorae at Los Barreros workshop, where other types —mainly Almagro 51C— were also produced (Bernal and Navas, 1998).

Figure 1. Location of the Baetican amphora workshops where the production of the type Dressel 23 has been attested (map data: Google, Instituto Geográfico Nacional). Illustration of the variants Dressel 23a and 23d (from Berni 1998 and Remolà 2000)

A first typological classification of the Dressel 23/Keay 13 variants was proposed by Keay (1984) and followed —with modifications— by Remolà (2000). An alternative and widely used classification is the one by Berni (1998), who differentiates the variants Dressel 23a (equivalent to Keay 13A),

Dressel 23b (Keay 13B and 12bis), Dressel 23c (including some Keay 13C amphorae, and the types Keay 14 and Tejarillo II) and Dressel 23d (comprising the majority of the Keay 13C amphorae as well as Keay 13D and 18). The definition of these typologies was based on the study of materials from consumption centres, mainly from the current Catalan area (*e.g.* Tarragona, Barcelona, Empúries). The most represented variants in these consumption centres are usually Dressel 23a and 23d (Figure 1); however, there are still significant gaps in the knowledge of the chronological span and the typological evolution of these variants during the Late Roman period (Berni and Moros, 2012a). Dressel 23a presents more formal similarities to the last variants of Dressel 20, and the hypothesis of Dressel 23 as a derivation from this last type is generally accepted (Remesal, 1983; Berni, 1998; Bernal, 2001; García Vargas and Bernal, 2008; Berni and Moros, 2012b). It is possible that the variant Dressel 23d was produced a bit later than the others, starting from the late 4th century (Berni and Moros, 2012b), although the two main variants Dressel 23a and 23d could have coexisted, as suggested by the archaeological evidence (*e.g.* Remolà, 2000).

Concerning the provenance of these amphorae, the examples attested in the Guadalquivir/Genil workshops belong mainly to the variant Dressel 23a. Conversely, the Dressel 23d variant has not been documented so far. It presents a quite different macroscopic fabric from the other variants, which shows similarities to some Almagro 51A-B and Almagro 51C amphorae (Keay, 1984; Berni, 1998; Remolà, 2000); for this reason, a possible production in the Baetican coast for this variant is suggested by Berni and Moros (2012b), a hypothesis that is not usually mentioned in the archaeological literature. The lack of published archaeometric studies for the Late Roman workshops in both the Guadalquivir/Genil and the Málaga areas (except for a preliminary report for this latter by Corrales *et al.*, 2011) does not help to solve this problem. The archaeological studies of Late Roman contexts from consumption centres tend to consider the Dressel 23 amphorae as an oil container mainly from the Guadalquivir/Genil area, while the possible imports of this type from the Málaga region are rarely mentioned and their relative significance remains unclear.

In order to tackle this issue, in this paper we present the archaeometric analysis of a series of Dressel 23 amphorae from consumption centres in the current Catalan coastal territory and, to a lesser degree, the Balearic Islands, these areas corresponding in the Late Roman period to the Hispanic provinces of *Tarraconensis* and *Balearica*, respectively. By means of an integrated chemical, mineralogical and petrographic approach, the aim is to examine the variety of fabrics and compositions that are represented in the consumption centres and investigate their provenance, providing new evidence on the production areas of the main Dressel 23 variants and, consequently, on the amphora trade between the *Baetica* and other Hispanic areas during the Late Roman period.

2. MATERIALS AND METHODS

The sampling was carried out on selected Late Roman contexts from three consumption centres in the *Tarraconensis* and one in the *Balearica* (Figure 2). The former include *Tarraco*/Tarragona —Vila-roma (TED'A, 1989; Remolà, 2000), Medieval Cathedral (Teixell *et al.*, 2005; Macias *et al.*, 2008) and Amphitheatre (Ciurana *et al.*, 2011, 2013)—, *Iluro*/Mataró —Carrer Sant Cristòfol nº 12 and Carrer Palau nº 32-34 (Cerdà *et al.*, 1997; Cela and Revilla, 2004)— and *Emporiae*/Sant Martí d'Empúries —Plaça Major (Aquilué and Burés, 1999)—. The Balearic samples come from the cistern found at the site of Sa Mesquida in Mallorca (Orfila, 1989; Buxeda *et al.*, 1998).

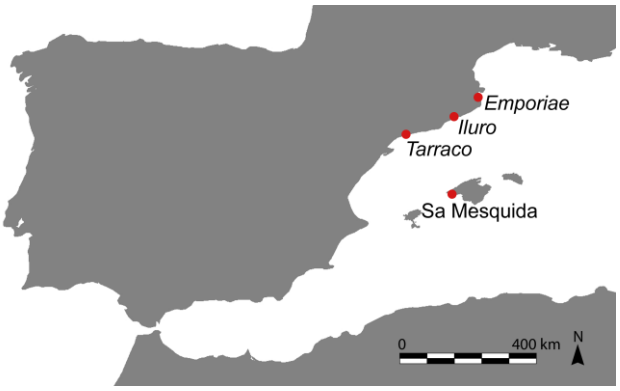

Figure 2. Location of the analysed consumption centres

Thirty amphora samples have been selected for archaeometric analysis (Table 1; Figure 3). The majority of them belong to Dressel 23 amphorae and include samples of the main variants of this type (Dressel 23a and 23d), as well as some other samples with a less clear attribution to any of the variants. A few samples can be classified as Dressel 23d similis, since they present the same macroscopic fabric as the Dressel 23d variant but with some morphological differences, a fact already noticed by Remolà (2000) for the samples from *Tarraco*. In addition to these samples, a number of amphorae belonging to other types (Almagro 51A-B mainly, and the indeterminate rim ABA002) were also analysed, due to their macroscopic similarities in fabric with the Dressel 23d samples. This would help verify if there is a possible compositional relationship between differ-

ent types of amphorae and help identify their provenance.

All samples were analysed using a combination of techniques, including optical microscopy (OM), X-ray diffraction (XRD) and X-ray fluorescence (XRF). Selected samples were also analysed through scanning electron microscope with energy dispersive X-ray spectroscopy (SEM-EDS).

The petrographic-mineralogical analysis of thin sections by means of OM was performed using an Olympus BX41 polarising microscope, working with a magnification between 20X and 200X, and equipped with a digital camera Olympus DP70. The identified fabrics were described following the system by Whitbread (1989, 1995) and Quinn (2013).

Table 1. List of the 30 amphora samples analysed in this study

Sample	*Amphora type*	*Archaeological context*	*Chronology of SU*
ABA001	Almagro 51A-B	*Tarraco*: Amphitheatre	5th-6th centuries
ABA002	Indeterminate rim	*Tarraco*: Amphitheatre	4th century
ABA003	Dressel 23d similis	*Tarraco*: Amphitheatre	5th-6th centuries
CAT208	Dressel 23a	*Tarraco*: Medieval Cathedral	500-550
CAT227	Dressel 23a	*Tarraco*: Medieval Cathedral	500-550
EMP301	Dressel 23a	*Emporiae*: Plaça Major	400-450 (esp. 400-425)
EMP318	Indeterminate rim (Dressel 23a?)	*Emporiae*: Plaça Major	6th century
EMP324	Dressel 23a	*Emporiae*: Plaça Major	6th century
ILU001	Dressel 23 (var. 23a?)	*Iluro*: Carrer Sant Cristòfol nº 12	300-325
ILU003	Dressel 23 (var. 23c?) / simile Tejarillo II	*Iluro*: Carrer Sant Cristòfol nº 12	300-325
ILU023	Dressel 23a	*Iluro*: Carrer Sant Cristòfol nº 12	475-535
ILU024	Dressel 23c	*Iluro*: Carrer Sant Cristòfol nº 12	475-535
ILU025	Almagro 51A-B	*Iluro*: Carrer Sant Cristòfol nº 12	475-535
ILU026	Almagro 51A-B	*Iluro*: Carrer Sant Cristòfol nº 12	475-535
ILU028	Dressel 23a or Tejarillo III	*Iluro*: Carrer Sant Cristòfol nº 12	475-535
ILU052	Dressel 23a	*Iluro*: Carrer Palau nº 32-34	450-500
ILU053	Dressel 23d similis	*Iluro*: Carrer Palau nº 32-34	After 450
MC0355	Dressel 23d similis	Sa Mesquida (Mallorca): Cistern	400-450
MC0356	Dressel 23d	Sa Mesquida (Mallorca): Cistern	400-450
MC0359	Dressel 23d	Sa Mesquida (Mallorca): Cistern	400-450
MC0387	Almagro 51A-B	Sa Mesquida (Mallorca): Cistern	400-450
MC0400	Almagro 51A-B	Sa Mesquida (Mallorca): Cistern	400-450
VIL063	Dressel 23d	*Tarraco*: Vila-roma	425-450/475
VIL064	Dressel 23d	*Tarraco*: Vila-roma	425-450/475
VIL065	Dressel 23a	*Tarraco*: Vila-roma	425-450/475
VIL066	Dressel 23a	*Tarraco*: Vila-roma	425-450/475
VIL067	Almagro 51A-B	*Tarraco*: Vila-roma	425-450/475
VIL076	Dressel 23d	*Tarraco*: Vila-roma	425-450/475
VIL077	Dressel 23d	*Tarraco*: Vila-roma	425-450/475
VIL078	Almagro 51A-B	*Tarraco*: Vila-roma	425-450/475

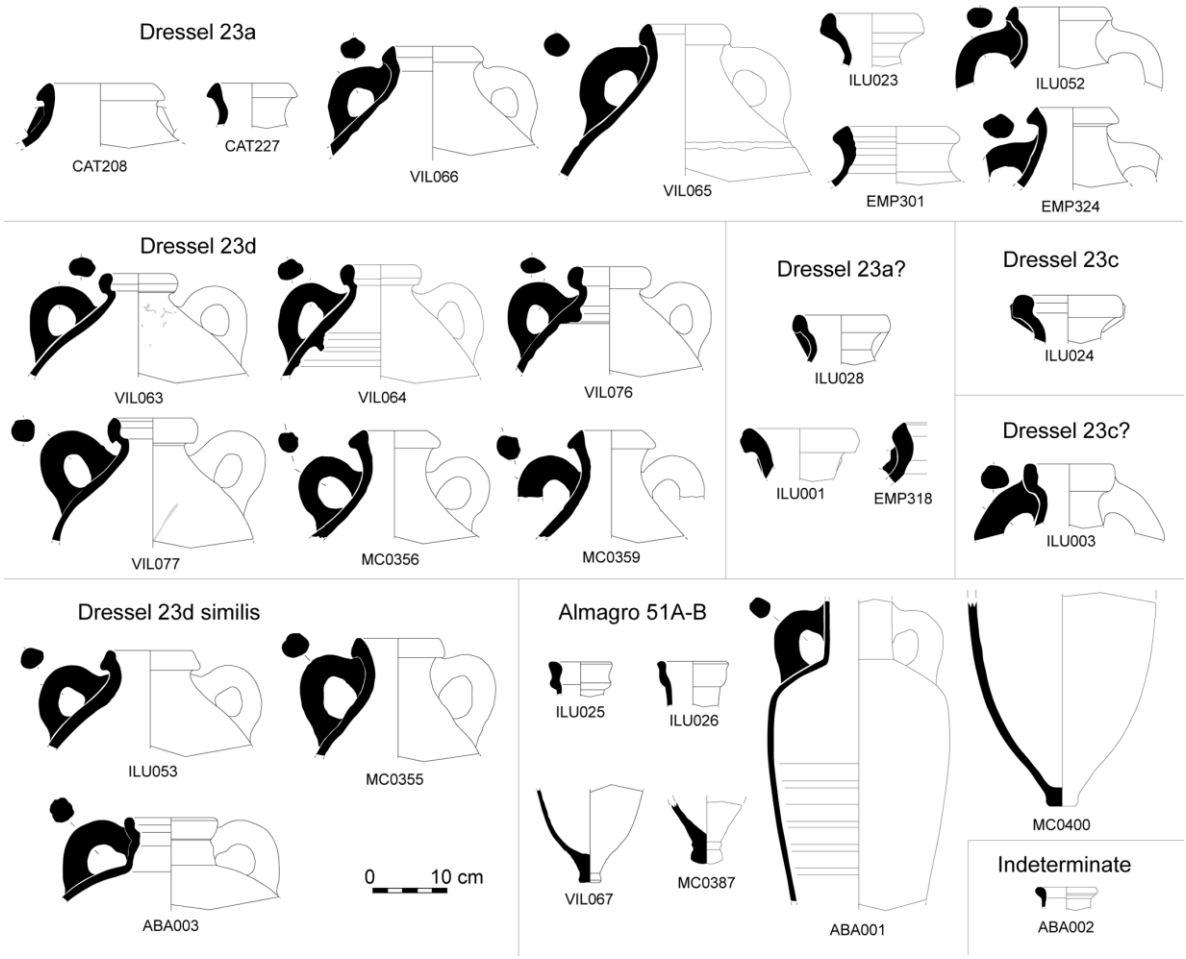

Figure 3. Illustrations of the amphorae analysed in this study (VIL, from TED'A 1989; ILU, from Cerdà et al. 1997 and Cela and Revilla 2004; EMP, from Aquilué and Burés 1999)

Further information on the mineralogical composition was obtained through XRD analysis, using a PANalytical X'Pert PRO MPD alpha 1 diffractometer. Spectra were taken from 5° to 80° 2θ, using a step-size of 0.026° and a step-time of 47.5 s. The crystalline phases were examined using the software High Score Plus by PANalytical, including the Joint Committee of Powder Diffraction Standards data bank.

The chemical composition of the samples was determined by means of XRF, using a Panalytical-Axios PW 4400/40 spectrometer (see for analytical routine Fantuzzi *et al*., 2015). This allowed for the determination of the following major, minor and trace elements: Fe_2O_3 (as total Fe), Al_2O_3, MnO, P_2O_5, TiO_2, MgO, CaO, Na_2O, K_2O, SiO_2, Ba, Rb, Nb, Pb, Zr, Y, Sr, Ce, Ga, V, Zn, Cu, Ni and Cr. A calibration line based on 60 International Geological Standards was used for quantifying the elemental concentrations. The obtained chemical data were transformed into additive log-ratios (alr) (Aitchison, 1986; Buxeda, 1999) and subjected to multivariate statistical treatment using the software S-PLUS 2000.

Fresh fracture surfaces of some samples were analysed through SEM-EDS, using a Quanta 200 FEI, XTE 325/D8395 scanning electron microscope equipped with an energy dispersive X-ray detector (working with a 20 kV accelerating voltage and a working distance of 10-14 mm). This allowed for the study of their microstructure and degree of vitrification, as well as the characterization of some mineral inclusions by means of chemical microanalysis.

3. RESULTS

3.1 Petrographic analysis

From the thin section OM analysis, four petrographic fabric (PF) groups represented by more than one sample can be differentiated, in addition to two fabrics represented by individual samples. A general distinction can be made between fabric groups (or fabrics) with sedimentary inclusions and a subordinated metamorphic component (PF 1 to 3) and others with a clear dominance of metamorphic rock fragments within their inclusions (PF 4 to 6).

Among the former, the most represented is PF 1 (samples CAT208, 227, VIL065, 066, EMP324,

ILU003, 023, 024, 028, 052) (Figure 4a-g), characterised by few inclusions (10-15%), usually not very coarse in size. These comprise calcareous inclusions (calcite and microfossils), monocrystalline quartz and a variable presence of alkali feldspars, micas (muscovite mainly), iron oxides, polycrystalline quartz and metamorphic rock fragments (phyllite, quartzmicaschist, quartzite, rare metagranitoid); accessory granitic rock fragments can also be found.

Based on the variable frequency of the subordinated components and on textural aspects, three fabrics can be differentiated in PF 1 (PF 1.1 to 1.3). PF 1.1 (VIL065, 066, EMP324, ILU024, 028) (Figure 4a) is the finest of the three, with a dominant fine fraction (<0.1 mm) of calcareous inclusions (calcite and microfossils), quartz and —at a lower frequency— micas and iron oxides; the coarse fraction (mode <0.3 mm) is scarce and consists of calcite, microfossils and quartz (monocrystalline mainly), other components being rare. PF 1.2 (CAT208, 227, ILU023, 052) (Figure 4b) is similar but has a more frequent coarse fraction (again with mode <0.3 mm) in which, besides the calcareous inclusions and monocrystalline quartz, other inclusions (metamorphic rock fragments, polycrystalline quartz and, to a lesser degree, alkali feldspars) are also frequent. PF 1.3 (ILU003) (Figure 4c) resembles PF 1.2 but shows an even more dominant coarse fraction and a slightly coarser mode of the calcareous inclusions and polycrystalline quartz (0.3-0.4 mm). Despite these differences, the nature of the inclusions is very similar in the three fabrics, *e.g.* the types of microfossils (foraminifera, ostracods, rare echinoids) and metamorphic rocks (Figure 4d-e), as well as the accessory components (chert, granitic rock fragments). They also show the same matrix, reddish brown to light brown in PPL, optically inactive (except VIL066 with low optical activity) and with clear evidence of clay mixing (streaks and pellets of both a reddish clay and a more calcareous one) (Figure 4f-g). In all the cases, the fabrics suggest tempering with a fine sand, moderately to well sorted.

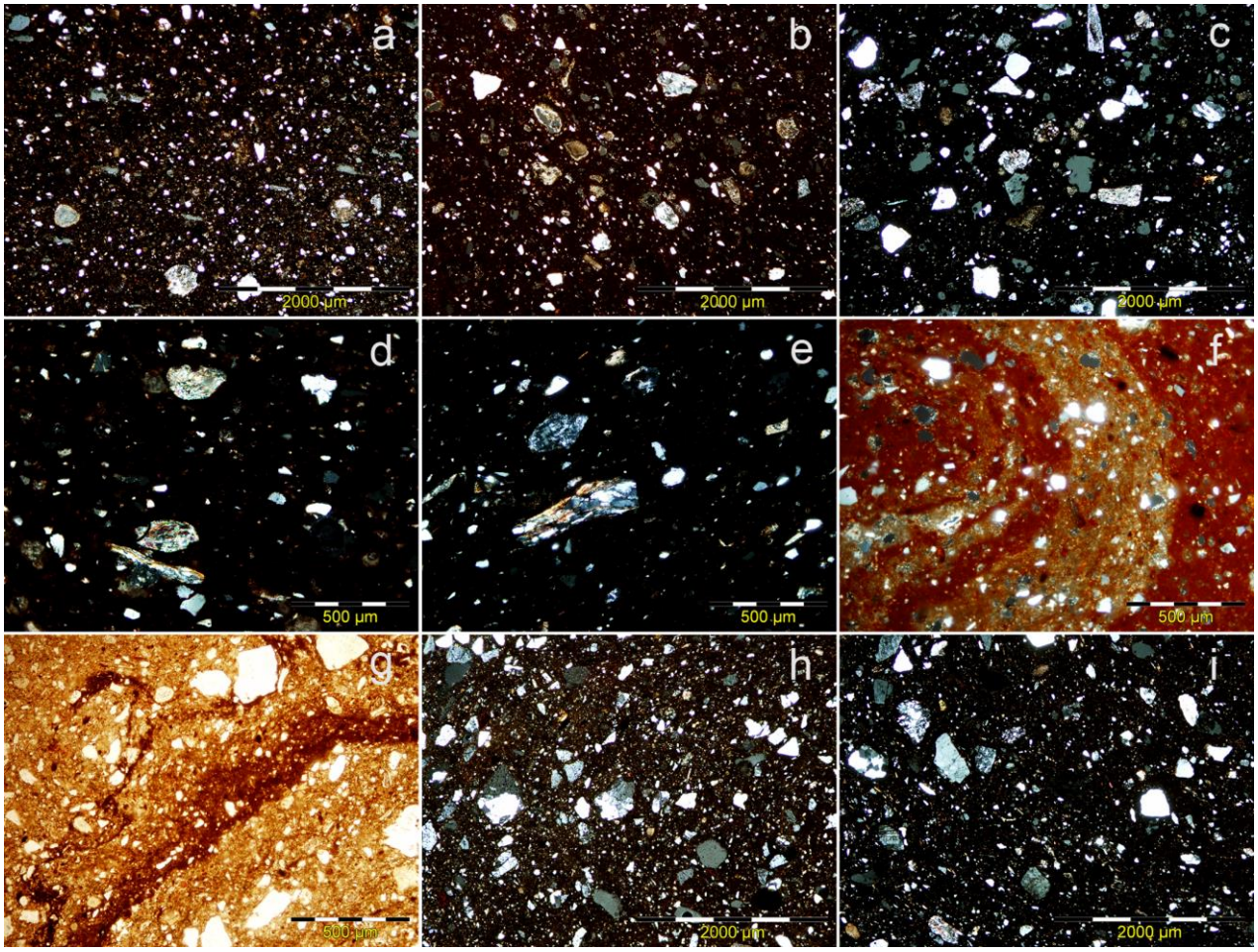

Figure 4. Microphotographs of thin sections from the petrographic fabric groups PF 1 (a-g), PF 2 (h) and PF 3 (i). (a) sample EMP324 (40x, XPL). (b) sample CAT208 (40x, XPL). (c) sample ILU003 (40x, XPL). (d) sample CAT227 (100x, XPL). (e) sample ILU023 (100x, XPL). (f) sample CAT208 (100x, XPL). (g) sample ILU028 (100x, PPL). (h) sample EMP301 (40x, XPL). (i) sample ILU001 (40x, XPL)

The fabric PF 2 (samples EMP301, 318) (Figure 4h) presents a bimodal distribution of the inclusions (20%), with a moderately sorted coarse fraction of quartz (mono- and polycrystalline), alkali feldspar and, to a lesser degree, plagioclase and metamorphic rock fragments (phyllite, quartzite, quartzmicaschist), usually not coarser than 0.3 mm. The fine fraction, comprising quartz, calcite and calcareous microfossils (foraminifera, ostracods, very rare echinoids) is abundant as well. Accessory fragments of granite and (very rare) basalt/trachyte are also observed. The clay matrix, brown to red coloured (PPL), displays low optical activity.

A particular fabric, PF 3 (Figure 4i), is found in the sample ILU001. It shows a bimodal distribution of the inclusions (15%). The fine/medium sandy coarse fraction, moderately sorted, consists of monocrystalline quartz and subordinated polycrystalline quartz, alkali feldspar, calcite and metamorphic rock fragments (metagranite, quartzite, schist), as well as accessory chert, plagioclase and rare granitoid rock fragments. The fine fraction is composed of quartz, micas (muscovite and biotite) and few calcareous inclusions; it is more micaceous than the fabrics in PF 1 and 2. An optically inactive, brown to orange-brown matrix (PPL) is observed.

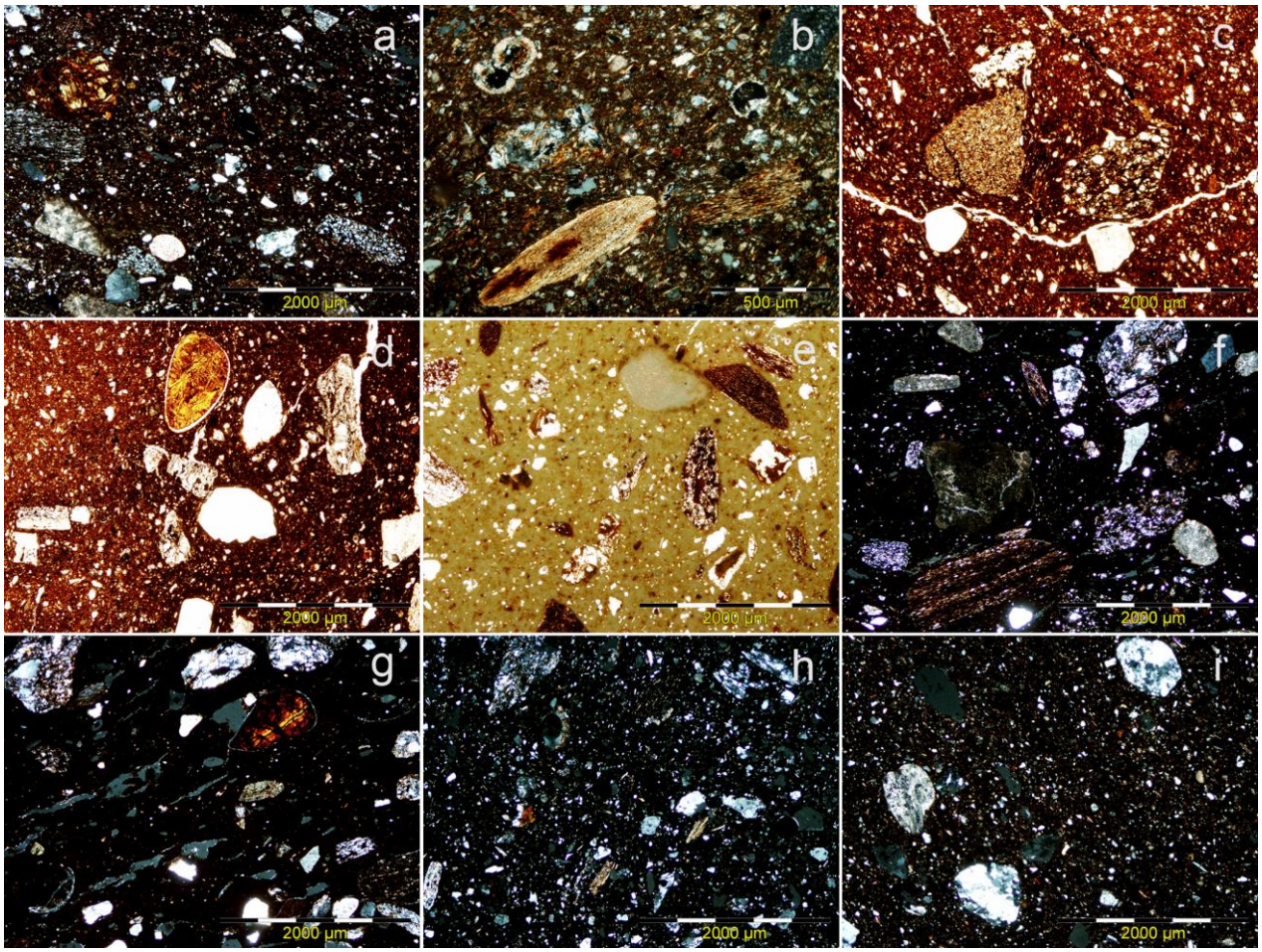

Figure 5. Microphotographs of thin sections from the petrographic fabric groups PF 4 (a-g), PF 5 (h) and PF 6 (i). (a) sample VIL066 (40x, XPL). (b) sample VIL077 (100x, XPL). (c-d) sample ILU026 (40x, PPL). (e) sample VIL078 (40x, PPL). (f) sample ABA001 (40x, XPL). (g) sample ABA003 (40x, XPL). (h) sample MC0359 (40x, XPL). (i) sample MC0356 (40x, XPL)

A very well represented fabric group is PF 4 (samples VIL063, 064, 067, 076, 077, 078, ABA001, 002, 003, ILU025, 026, 053, MC0355, 400) (Figure 5a-g), characterised by a clear bimodal distribution of the inclusions (15-30%), with a predominant poorly sorted coarse fraction (>0.25 mm), mainly with coarse to very coarse sand. This comprises dominant, heterogeneous metamorphic rock fragments (phyllite, schist, quartzite, meta-argillite; very rare gneiss, marble, amphibolite), as well as a subordinated presence of fine-grained sedimentary rock fragments (argillite, mudstone), quartz (mono- and polycrystalline) and calcareous inclusions (limestone and microfossils). Accessory components of the coarse fraction are sandstone fragments, chert, biotite and, occasionally, ophiolitic inclusions (serpen-

tine and semi-altered ortho- and clinopyroxene). The fine fraction (mode <0.1 mm) is usually abundant and comprises quartz, micas (muscovite mainly), calcareous inclusions —with frequent microfossils (ostracods, foraminifera, very rare echinoids)— and iron oxides.

The majority of the samples in this group show a same fabric, PF 4.1 (Figure 5a-e), with a mode of 0.5-0.8/1.2 mm for the coarse fraction. The matrix in this fabric, optically inactive or with low optical activity, is usually reddish brown in PPL (Figure 5c-d) except in higher fired samples with a greenish brown or green-grey colour (Figure 5e). Another exception is the sample MC0400, with a low-fired matrix that displays high optical activity and shows, in PPL, an orange-brown core and greenish brown surfaces. In a few samples, fine streaks and pellets of two different clays suggest a clay mixing process.

Three samples in this group (ABA001, 002, 003) do not belong to PF 4.1 and each present a different fabric (PF 4.2 to 4.4, respectively). PF 4.2 (Figure 5f) shows a coarser texture, with a coarse fraction mode between 0.8-1.0 mm and contains a higher frequency of very coarse sand (>1 mm) than the first fabric, while the fine fraction is scarcer and comprises quartz and micas (muscovite mainly), but with very few calcareous inclusions. In PF 4.3, the fine fraction is similar to the one in PF 4.1, although the clay matrix is clearly more iron-rich (no clay mixing is observed); the mode of the coarse fraction is finer than in the other fabrics (0.4-0.6 mm). Finally, PF 4.4 (Figure 5g) is clearly differentiated by a much scarcer (almost absent) fine fraction of silt and very fine sand (muscovite and quartz, the calcareous inclusions being rare) and an iron-rich clay matrix; the coarse fraction is similar to PF 4.1 with minor differences in texture and in the frequency of some inclusions (*e.g.* higher frequency of alkali feldspar; more ostracods in the coarse fraction; serpentine slightly more visible).

Other less represented metamorphic fabric groups are PF 5 and PF 6. In PF 5 (samples MC0359, 387) (Figure 5h) the inclusions (20%) comprise an abundant fine fraction (mode <0.1 mm) of quartz and micas (muscovite) mainly, and a subordinated coarse fraction (>0.25 mm) dominated by metamorphic rock fragments (schist, phyllite, quartzite, some metargillites, rare amphibolite) and common quartz (mono- and polycrystalline), while other inclusions (*e.g.* limestone, argillite) are accessory. The two samples may represent different fabrics, since in MC0387 the coarse fraction shows a clearly higher mode (0.50-0.75 mm) than in MC0359 (0.25-0.50 mm). The matrix is brown (PPL) and optically inactive.

The fabric PF 6 is observed only in the sample MC0356 (Figure 5i). The inclusions (20%) show an abundant fine fraction (mode <0.1 mm) of quartz, micas (muscovite and biotite) and calcite, and a less frequent coarse fraction (>0.25 mm) with dominant metamorphic rock fragments (quartzite and schist mainly; also some phyllite and marble) and common quartz (mainly polycrystalline). A distinctive feature of this fabric is the subordinated presence of garnet and staurolite inclusions, in addition to accessory kyanite and andalusite. The matrix is orange-brown (surfaces) to light greenish brown (core) in PPL, with low optical activity in XPL.

3.2 Chemical analysis

The normalised chemical results for the 30 analysed individuals (Table 2) suggest that a certain compositional heterogeneity is present in the data set. The calculation of the variation matrix τ.i indicates the variation introduced by this element into the data set (a high τ.i value indicates a high variation associated with this element "i"). (Aitchison, 1986, 1992; Buxeda and Kilikoglou, 2003). Here it indicates that these variations are mainly associated with differences in Cu (τ.Cu = 3.76), P_2O_5 (τ.P_2O_5 = 3.19), CaO (τ.CaO = 2.87) and Ba (τ.Ba = 2.19). The obtained value for the total variation (0.73) may be indicative of a polygenic sample (Buxeda and Kilikoglou, 2003).

A cluster analysis of the data obtained by XRF was performed, after an additive log-ratio transformation (alr) of the concentrations using SiO_2 as a divisor (P_2O_5 and Pb were not included in this analysis due to possible contamination problems). Two main groups (A and B) can be differentiated in the resulting dendrogram (Figure 6), each with a certain internal variability. These general groups are also observed in the biplot of the first two principal components of the PCA in Figure 7, both together accounting for 63% of the total variance. The differences between both groups are related to variations in a series of elements (mainly Cu, Ba, Na_2O, K_2O, Rb, Cr, V, Sr), as can be inferred from the PCA and the chemical data (Table 2); they both show an internal variability concerning their CaO percentages.

The comparison of the chemical results with the petrographic fabric groups reveals a good correspondence, as seen in Figure 6. The chemical group A comprises the samples that form the fabric groups PF 1 and 2, each associated with separate clusters in the dendrogram due to minor chemical differences between them (Table 3). With regard to the fabric group PF 1, no significant chemical differences are observed between the fabrics PF 1.1 and 1.2, but the fabric PF 1.3 —represented only by the sample ILU003— is slightly differentiated in chemical composition from the other samples of the group (Figure 6-7; Table 2).

Table 2. Normalised chemical results of the amphora samples obtained by XRF. Concentrations of major and minor oxides are in %, other minor and trace elements are in ppm

Sample	*Fe_2O_3*	*Al_2O_3*	*MnO*	*P_2O_5*	*TiO_2*	*MgO*	*CaO*	*Na_2O*	*K_2O*	*SiO_2*
ABA001	6.53	15.99	0.10	0.18	0.75	2.65	9.81	0.68	2.82	60.30
ABA002	6.28	16.20	0.07	0.22	0.85	2.75	6.73	0.79	3.08	62.85
ABA003	7.23	17.44	0.10	0.17	0.77	2.60	6.44	0.71	3.20	61.17
CAT208	6.28	14.29	0.05	0.42	0.76	2.68	12.19	0.79	2.35	60.04
CAT227	6.29	14.10	0.05	0.33	0.75	2.70	14.67	0.51	2.19	58.26
EMP301	5.52	13.42	0.04	0.42	0.71	2.31	11.33	0.66	2.61	62.84
EMP318	5.60	13.57	0.04	0.41	0.71	2.22	11.25	0.66	2.51	62.90
EMP324	6.12	14.64	0.05	0.51	0.77	2.78	13.90	0.56	2.27	58.25
ILU001	5.26	16.53	0.05	0.24	0.66	1.70	11.73	0.69	3.36	59.62
ILU003	6.39	16.00	0.06	0.34	0.82	2.37	8.63	0.54	2.73	61.98
ILU023	6.42	16.02	0.07	0.30	0.81	2.73	11.79	0.53	2.46	58.74
ILU024	6.32	15.08	0.05	0.30	0.78	2.61	13.71	0.52	2.34	58.14
ILU025	5.98	14.80	0.07	0.41	0.75	2.55	10.83	0.83	3.03	60.60
ILU026	5.87	14.13	0.10	0.28	0.69	2.66	11.84	0.79	2.95	60.55
ILU028	6.11	15.07	0.05	0.28	0.75	2.95	13.31	0.54	2.53	58.25
ILU052	6.67	16.44	0.05	0.29	0.84	2.40	11.51	0.61	2.59	58.46
ILU053	6.38	15.45	0.07	0.47	0.77	2.56	10.63	0.89	3.11	59.51
MC0355	5.87	15.04	0.06	0.38	0.77	2.58	10.21	1.16	3.02	60.78
MC0356	5.99	16.93	0.10	0.51	0.79	2.35	7.20	0.89	3.00	62.11
MC0359	6.20	15.65	0.07	0.27	0.89	2.65	6.26	0.91	3.04	63.91
MC0387	5.88	15.68	0.06	0.44	0.86	2.53	6.58	0.99	3.15	63.68
MC0400	5.03	13.12	0.06	0.73	0.71	2.46	14.66	0.81	2.85	59.42
VIL063	5.70	14.59	0.07	0.40	0.74	2.40	13.89	0.89	3.13	58.03
VIL064	5.72	14.68	0.06	0.29	0.77	2.44	11.60	0.79	3.15	60.35
VIL065	5.74	13.81	0.04	0.29	0.74	2.52	17.46	0.61	2.18	56.46
VIL066	6.19	14.35	0.05	0.36	0.77	2.63	13.71	0.58	2.47	58.74
VIL067	5.52	13.83	0.07	0.31	0.72	2.60	14.32	0.79	2.89	58.81
VIL076	5.69	14.26	0.06	0.26	0.74	2.60	12.41	0.91	3.31	59.62
VIL077	5.52	14.12	0.06	0.30	0.75	2.45	11.95	0.91	3.10	60.68
VIL078	5.40	13.51	0.06	0.28	0.72	2.79	13.82	0.94	2.58	59.77

Sample	*Ba*	*Rb*	*Nb*	*Pb*	*Zr*	*Y*	*Sr*	*Ce*	*Ga*	*V*	*Zn*	*Cu*	*Ni*	*Cr*
ABA001	674	112	15	32	161	27	243	65	19	116	83	45	52	108
ABA002	458	120	17	41	195	29	273	75	19	117	95	46	44	96
ABA003	589	125	16	38	147	27	230	72	21	127	83	47	53	109
CAT208	290	92	17	21	195	24	418	66	18	141	85	21	33	128
CAT227	279	84	17	24	183	23	332	65	17	144	77	18	32	122
EMP301	351	86	16	21	165	21	289	59	16	126	78	36	28	117
EMP318	294	85	15	18	169	22	290	62	17	130	75	21	29	112
EMP324	239	90	18	18	184	24	346	57	18	133	86	21	34	131
ILU001	669	141	12	43	172	29	195	64	19	89	82	25	27	73
ILU003	336	103	16	35	178	24	266	70	20	149	92	20	35	124
ILU023	279	99	15	21	172	24	306	59	20	144	94	20	35	127
ILU024	335	92	15	20	179	23	301	68	19	145	90	16	33	124
ILU025	447	110	14	22	190	27	267	59	18	104	88	27	43	93
ILU026	444	104	13	29	169	26	244	63	18	107	89	33	43	89
ILU028	398	92	15	20	173	23	288	68	19	141	86	14	32	118
ILU052	300	105	17	21	175	24	283	76	21	158	100	16	43	133

ILU053	536	121	15	24	186	29	259	70	20	119	91	32	44	101
MC0355	389	118	16	24	189	26	295	75	19	94	97	29	41	114
MC0356	303	102	15	22	166	23	202	62	18	112	112	23	36	118
MC0359	368	116	17	31	196	26	228	87	19	97	106	27	39	116
MC0387	405	119	17	25	206	27	247	78	19	104	104	25	38	123
MC0400	379	97	14	24	177	24	283	65	17	100	112	39	37	135
VIL063	407	109	15	33	176	26	298	67	17	115	79	48	41	98
VIL064	377	112	15	35	182	26	263	63	18	102	86	48	41	97
VIL065	262	88	17	23	183	22	391	62	17	138	79	23	31	131
VIL066	242	86	17	22	187	23	317	68	17	149	85	27	31	112
VIL067	336	100	15	35	170	26	263	57	16	103	82	53	42	93
VIL076	342	104	15	24	171	25	243	62	17	104	78	40	40	87
VIL077	407	104	15	27	183	25	380	53	16	103	81	45	38	89
VIL078	348	95	14	27	174	24	282	58	16	84	75	35	37	110

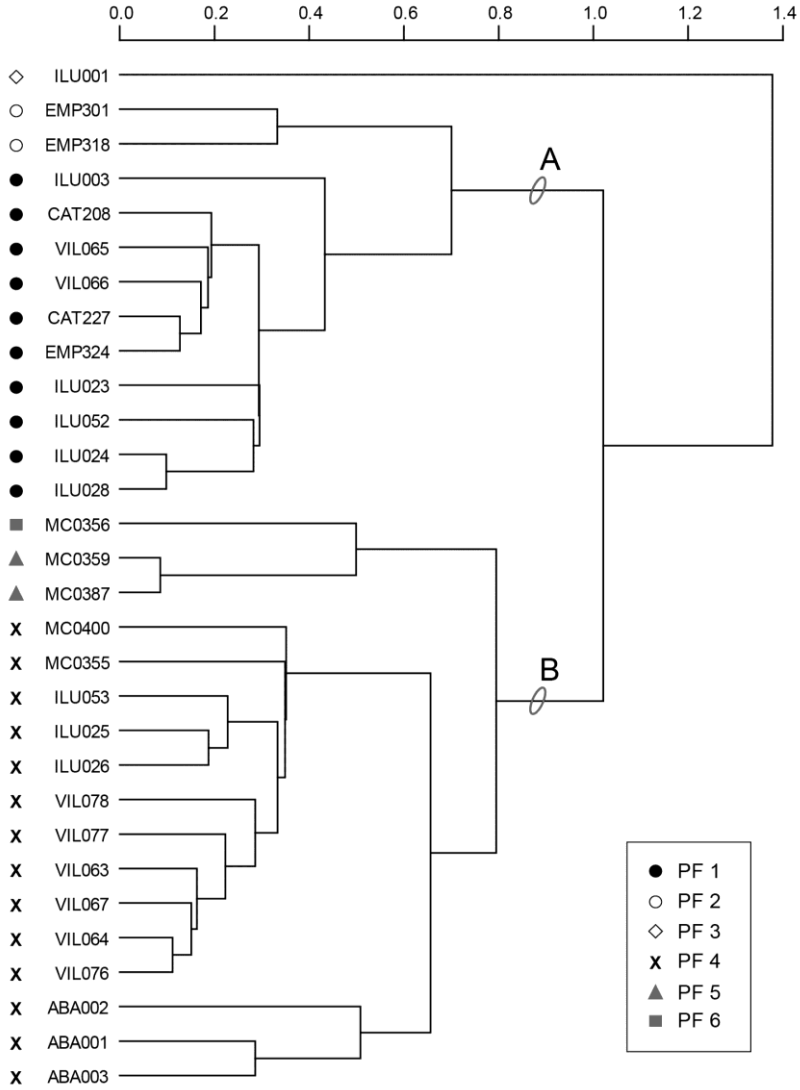

Figure 6. Dendrogram resulting from a cluster analysis (using the centroid agglomerative method and the squared Euclidean distance) on the 30 amphora samples analysed by XRF, based on the subcomposition Fe_2O_3, Al_2O_3, MnO, TiO_2, MgO, CaO, Na_2O, K_2O, Ba, Rb, Nb, Zr, Y, Sr, Ce, Ga, V, Zn, Cu, Ni and Cr; SiO_2, was used as a divisor in the log-ratio transformation of the data. Two main chemical groups (A and B) can be defined. The petrographic fabric (PF) for each sample is indicated

The chemical group B corresponds well with the fabric groups characterised by a dominant metamorphic composition (PF 4 to 6), showing chemical differences between them that are visible in the cluster tree (Figure 6). The fabrics PF 5 and 6 have in general a lower content of CaO, Sr and Cu and higher of Zn than the large group PF 4 (Figure 7; Table 3). Concerning the group PF 4, the most represented fabric, PF 4.1, presents a homogeneous chemical composition, forming a separate cluster in Figure 6 from the other fabrics of the group (PF 4.2, 4.3 and 4.4). These latter —samples ABA001, 002 and 003, respectively— present lower CaO percentages than PF 4.1, in addition to other minor differences (Table 2); the CaO content is particularly lower in PF 4.3 and 4.4, that must be associated with the iron-rich clay matrix observed in thin section for these samples, without the clay mixing and the fine calcareous inclusions documented in PF 4.1.

The sample ILU001, which is the only individual in the petrographic fabric PF 3, behaves as a chemical loner (Figure 6), with lower MgO and higher K_2O, Rb and Ba than the other samples in the data set (Table 3).

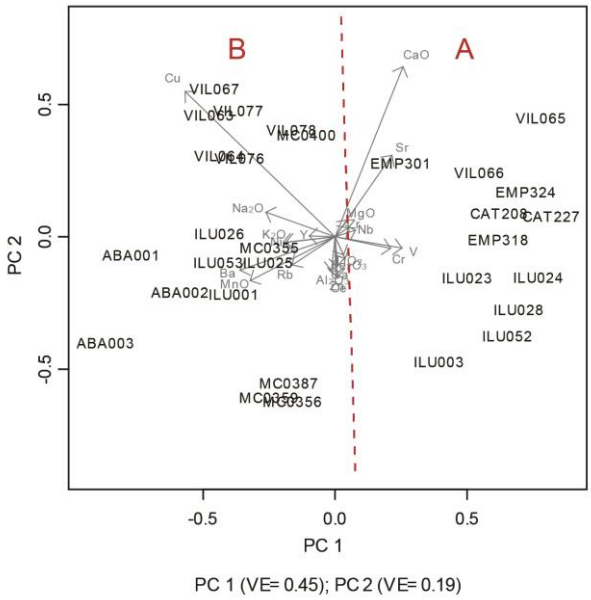

Figure 7. PCA of the alr-transformed chemical data for the 30 amphora samples. Biplot PC1-PC2, based on the same subcomposition as the cluster tree in Figure 6; the two main chemical groups (A and B) defined from the cluster analysis are indicated here in the biplot. The analysis was performed on the covariance matrix

Table 3. Mean chemical composition of the six petrographic fabric groups (PF). Mean (m) and standard deviation (sd) values are presented for each element

	PF 1 (n=10)		*PF 2 (n=2)*		*PF 3 (n=1)*	*PF 4 (n= 14)*		*PF 5 (n= 2)*		*PF 6 (n=1)*
	m	*sd*	*m*	*sd*		*m*	*sd*	*m*	*sd*	
(%)										
Fe_2O_3	6.25	0.24	5.56	0.05	5.26	5.91	0.55	6.04	0.23	5.99
Al_2O_3	14.98	0.91	13.49	0.10	16.53	14.80	1.16	15.66	0.02	16.93
MnO	0.05	0.01	0.04	0.00	0.05	0.07	0.02	0.07	0.01	0.10
P_2O_5	0.34	0.07	0.41	0.00	0.24	0.33	0.14	0.35	0.12	0.51
TiO_2	0.78	0.03	0.71	0.00	0.66	0.75	0.04	0.88	0.02	0.79
MgO	2.64	0.17	2.27	0.06	1.70	2.58	0.11	2.59	0.09	2.35
CaO	13.09	2.31	11.29	0.05	11.73	11.37	2.54	6.42	0.23	7.20
Na_2O	0.58	0.08	0.66	0.00	0.69	0.85	0.12	0.95	0.06	0.89
K_2O	2.41	0.18	2.56	0.07	3.36	3.02	0.19	3.09	0.08	3.00
SiO_2	58.73	1.44	62.87	0.04	59.62	60.17	1.15	63.79	0.17	62.11
(ppm)										
Ba	296	49	323	40	669	438	99	386	26	303
Rb	93	7	86	1	141	109	9	117	2	102
(ppm)										
Nb	16	1	15	0	12	15	1	17	0	15
Pb	23	5	19	2	43	30	6	28	4	22
Zr	181	7	167	3	172	177	13	201	7	166
Y	23	1	21	0	29	26	2	26	1	23
Sr	325	49	290	1	195	273	37	237	13	202
Ce	66	6	61	2	64	65	7	82	6	62
Ga	19	1	16	0	19	18	2	19	0	18
V	144	7	128	3	89	107	11	101	5	112
Zn	87	7	76	2	82	87	10	105	2	112
Cu	20	4	29	11	25	40	8	26	1	23
Ni	34	3	28	1	27	43	5	39	1	36
Cr	125	7	115	3	73	101	13	119	5	118

3.3 XRD mineralogical analysis

The XRD results provide further information on the mineralogical composition of each sample, including primary phases as well as any possible firing and secondary phases; this composition allows for a first estimation of the equivalent firing temperatures (EFT, see Roberts, 1963; Maggetti, 1982; Cultrone *et al*., 2001; Buxeda and Cau, 2004; Maggetti *et al*., 2011) (Table 4).

Some of the fabrics defined through the petrographic study, each showing an homogeneous chemical composition, comprise samples with differences in their macroscopic colour and texture. The XRD spectra reveal that these differences may be associated —at least partially— with EFT variations within each fabric. This is more evident for the fabric group PF 4 and, in particular, for the fabric PF 4.1, in which the lower fired samples present a red-orange colour (sometimes with yellowish surfaces) to the naked eye, that tends to change into a yellowish cream to light orange colour with the increase of the firing temperatures, in addition to a clear textural change (Figure 8).

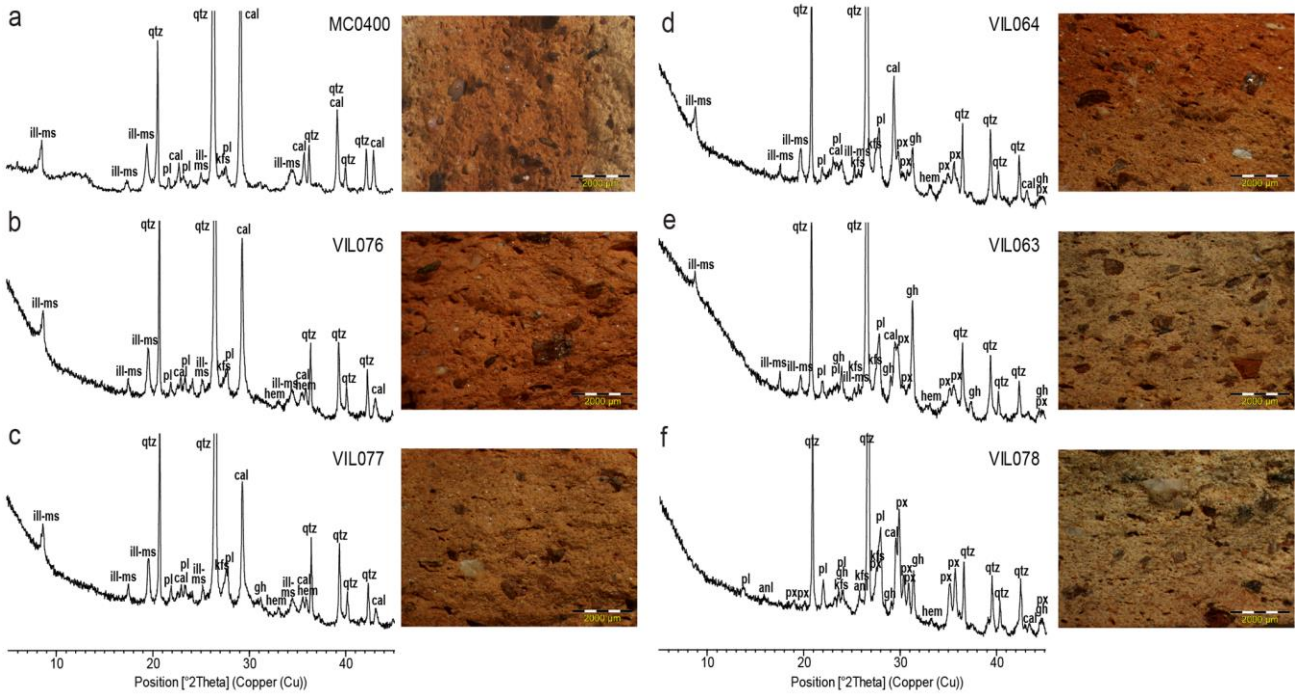

Figure 8. XRD spectra for selected samples of the fabric PF 4.1, along with photographs for each sample (taken at 15x) showing macroscopic changes related to increasing firing temperatures from (a) to (f). Abbreviations for minerals (based on Kretz, 1983): qtz, quartz; pl, plagioclase; kfs, K-feldspar; cal, calcite; gh, gehlenite; px, pyroxene; hem, hematite; ill-ms, illite-muscovite; anl, analcime

It is worth mentioning that the XRD spectra for the sample VIL078 (PF 4.1) reveal the presence of small peaks of analcime (Figure 8), a sodic zeolite usually related to post-depositional alteration of a vitreous phase in calcareous ceramics (Buxeda *et al*., 2002; Schwedt *et al*., 2006). This may be associated with the lower concentrations of K_2O and Rb and the slightly higher Na_2O observed in this sample when compared to the other samples of the same fabric (Table 2).

Concerning the fabric group PF 1, each of the two main fabrics PF 1.1 and 1.2 include well-fired samples (EFT 850-950ºC) and one sample with a slightly over-fired (EFT ≥950/1000ºC), as well as a lower fired sample (VIL066) in PF 1.1 (EFT ~850ºC, see Table 4). These differences in firing temperature are reflected in the macroscopic aspect and texture of the fabrics (Figure 9), even if in all the cases the fabric is heterogeneous to the naked eye (from reddish to yellowish hues), with differences between core and surfaces and, in some of the samples, variations related to the incomplete mixing of two clays that is clearly seen in thin section. Some high-fired samples show calcite peaks in XRD that may be associated with secondary calcite (Figure 9); this is more evident for a few samples (VIL065, EMP324) in which abundant secondary calcite (mainly as microcrystalline calcite scattered in the matrix) was also observed in the OM thin section analysis.

Table 4. Mineralogical composition and equivalent firing temperature (EFT) of the 30 amphora samples, determined from XRD. The samples are organised by fabric, based on the results of the OM analysis. Tr.: trace. Abbreviations for minerals (based on Kretz, 1983): Qtz, quartz; Pl, plagioclase; Kfs, K-feldspar; Cal, calcite; Gh, gehlenite; Px, pyroxene; Hem, hematite; Ill-Ms, illite-muscovite; Anl, analcime

	Sample	*Qtz*	*Pl*	*Kfs*	*Cal*	*Gh*	*Px*	*Hem*	*Ill-Ms*	*Anl*	*EFT (ºC)*
PF 1											
	PF 1.1										
	VIL065	+	+	+	+	+	+	+			≥ 950/1000
	VIL066	+	+	+	+	Tr.		+	+		~850
	EMP324	+	+	+	+	+	+	+	+		850-950
	ILU024	+	+	+	+	+	+	+	+		850-950
	ILU028	+	+	+	+	+	+	Tr.	+		850-950
	PF 1.2										
	CAT208	+	+	+	+	+	+	+	+		850-950
	CAT227	+	+	+	+	+	+	+	+		850-950
	ILU023	+	+	+	+	+	+	+			≥ 950/1000
	ILU052	+	+	+	+	+	+	+	+		850-950
	PF 1.3										
	ILU003	+	+	+	+	+	+	+	+		850-950
PF 2											
	EMP301	+	+	+	+	Tr.	+	Tr.	+		850-950
	EMP318	+	+	+	+	+	+	Tr.	+		850-950
PF 3											
	ILU001	+	+	+	+	+	+	Tr.	+		850-950
PF 4											
	PF 4.1										
	VIL063	+	+	+	+	+	+	Tr.	+		850-950
	VIL064	+	+	+	+	+	+	+	+		850-950
	VIL067	+	+	+	+	+	+	+	+		850-950
	VIL076	+	+	+	+			+	+		≤ 800/850
	VIL077	+	+	+	+	+	Tr.?	+	+		850-900
	VIL078	+	+	+	+	+	+	Tr.		Tr.	≥ 950/1000
	ILU025	+	+	+	+	+	+	+	+		850-950
	ILU026	+	+	+	+	Tr.		+	+		~850
	ILU053	+	+	+	+	+	+	Tr.	+		850-950
	MC0355	+	+		+	+	+	+	+		850-950
	Sample	*Qtz*	*Pl*	*Kfs*	*Cal*	*Gh*	*Px*	*Hem*	*Ill-Ms*	*Anl*	*EFT (ºC)*
PF 4											
	MC0400	+	+	+	+				+		≤ 800/850
	PF 4.2										
	ABA001	+	+	+	+	+	+	+	+		850-950
	PF 4.3										
	ABA002	+	+	+	+	+	+	+	+		850-950
	PF 4.4										
	ABA003	+	+	+	+	+	+	+	+		850-950
PF 5											
	MC0359	+	+	+	+	+	+	+	+		850-950
	MC0387	+	+		+	+	+	+	+		850-950
PF 6											
	MC0356	+	+	+	+				+		≤ 800/850

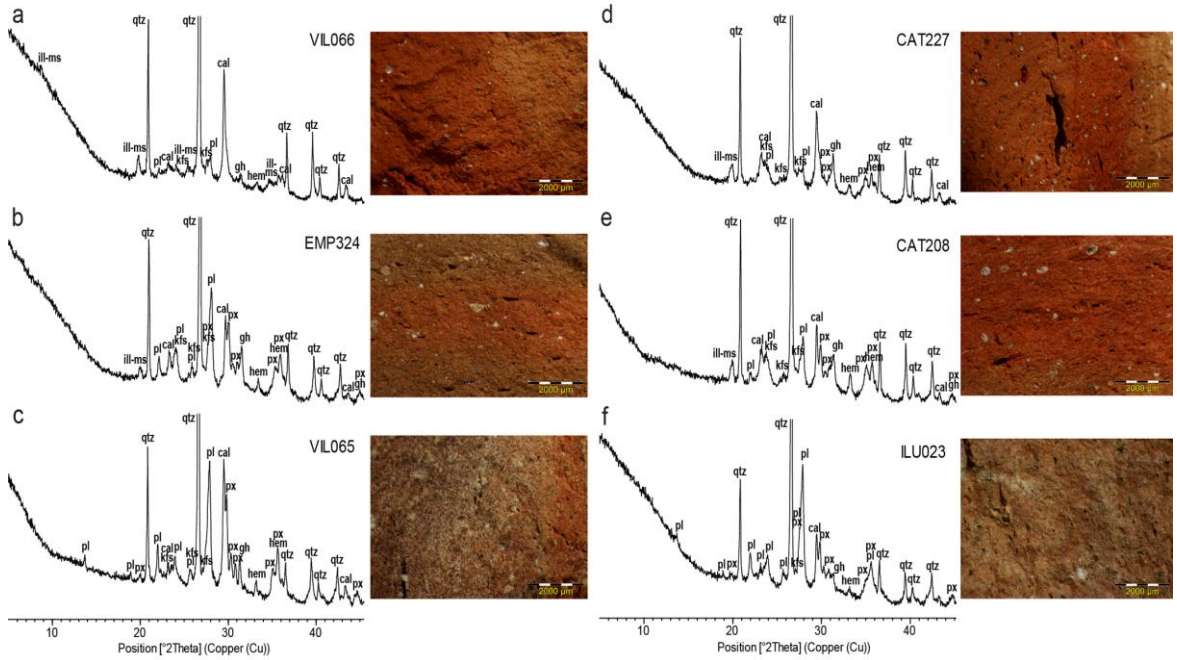

Figure 9. XRD spectra for selected samples of the fabrics PF 1.1 (a-c) and PF 1.2 (d-f), along with photographs for each sample (taken at 15x) showing macroscopic changes related to increasing firing temperatures from (a) to (c) and from (d) to (f). Abbreviations for minerals (based on Kretz, 1983): qtz, quartz; pl, plagioclase; kfs, K-feldspar; cal, calcite; gh, gehlenite; px, pyroxene; hem, hematite; ill-ms, illite-muscovite

The less represented fabrics in the data set (PF 2, 3, 5, 6) usually present firing phases that suggest an EFT between 850-950ºC, except PF 6 where the only analysed sample (MC0356) is related to low firing temperatures (≤800/850ºC) (Table 4).

3.4 SEM-EDS analysis

Representative samples of the main fabrics (PF 1.1, 1.2 and 4.1) were analysed under SEM-EDS in order to examine the microstructural changes of the matrix related to differences in the firing temperatures and to obtain a more precise determination of the EFTs (Maniatis and Tite, 1981; Tite *et al*., 1982), thus complementing the information provided by XRD. A comparison with the sintering and vitrification stages defined by Maniatis and Tite (1981) can be made, taking into account that the samples in the three fabrics are all calcareous (with CaO percentages between 10-17%) and fired in a reducing/oxidising atmosphere.

For the fabric PF 1.1, samples with initial vitrification (VIL066), extensive vitrification (EMP324) and very extensive vitrification with fine bloating pores (VIL065) are observed (Figure 10). This may suggest firing temperatures of around 800-850ºC for the first sample and between 850-1050ºC for the two latter samples, however in VIL065 the temperature was much closer to 1050ºC while in EMP324 it probably was not higher than 950ºC. Three analysed samples of the fabric PF 1.2 (CAT208, CAT227, ILU023) show extensive vitrification, however ILU023 shows a very advanced stage of vitrification comparable to VIL065 for the first fabric, while in CAT208 and CAT227 the microstructure more resembles the microstructure found in EMP324.

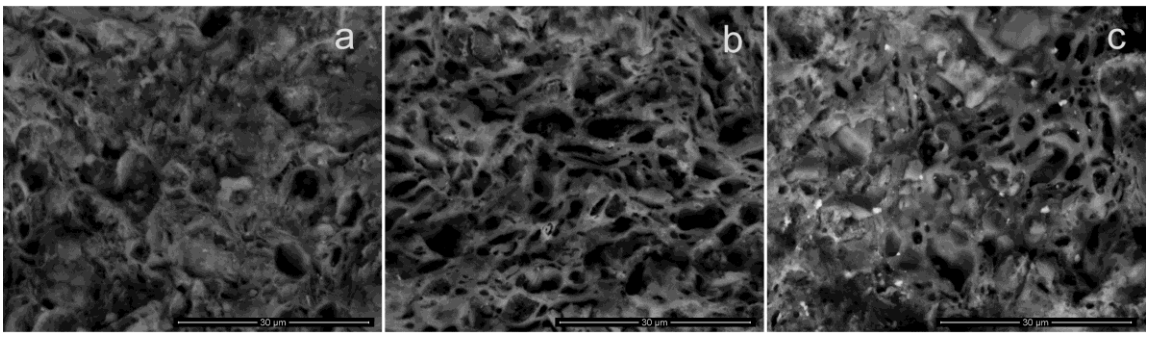

Figure 10. SEM microphotographs of the fabric PF 1.1, all taken at the same magnification (5000x). (a) sample VIL066, initial vitrification. (b) sample EMP324, extensive vitrification. (c) sample VIL065, very extensive vitrification

As for the fabric PF 4.1, some samples have been observed with no vitrification (VIL076, MC0400), related to firing temperatures under 800ºC, as well as samples with initial vitrification (ILU026), extensive vitrification (VIL063, VIL064) and very extensive vitrification (VIL078) (Figure 11a-d). Chemical microanalysis under SEM-EDS also reveals the very rare presence, in some of these samples (VIL063, VIL064), of monazite particles (Figure 11e). This rare mineral is usually present as an accessory component in some igneous rocks (granite, pegmatite) and metamorphic rocks, in particular schist, gneiss, migmatite and intermediate- to high-grade rocks derived from argillaceous sediments (Overstreet, 1967; Hurlbut and Klein, 1993). These monazite inclusions are absent in the analysed samples of the fabric group PF 1.

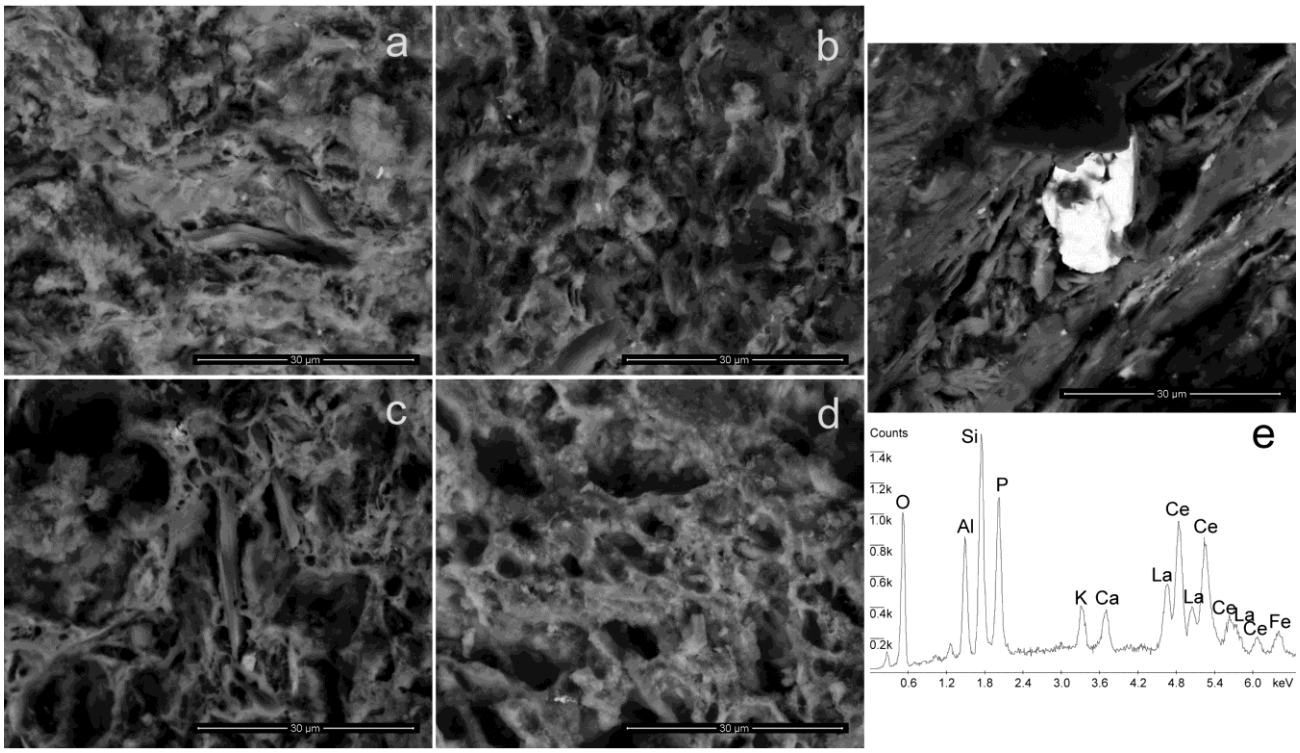

Figure 11. SEM microphotographs of the fabric PF 4.1, all taken at the same magnification (5000x). (a) sample VIL076, no vitrification. (b) sample ILU026, initial vitrification. (c) sample VIL064, extensive vitrification. (d) sample VIL078, very extensive vitrification. (e) sample VIL063, microphotograph and EDAX spectra of a monazite inclusion

4. DISCUSSION

The results of the archaeometric analyses in this study indicate the presence of a series of fabric groups and individual fabrics that are associated with well-differentiated chemical and petrographic compositions. From the integration of the typological evidence of the 30 analysed samples, it can be noticed that the fabric groups PF 1 and 2 include all the examples that belong to the variant Dressel 23a and the few samples related to the variant Dressel 23c. The fabric PF 3 comprises only one sample (ILU001) that is possibly related —with some doubt— to the variant Dressel 23a. Conversely, all the analysed amphorae classified as Dressel 23d (and 23d similis) and Almagro 51A-B/Keay 19A-B are included in the fabric groups PF 4 to 6.

Despite the absence of archaeometric reference groups from the production centres, the possible provenance for these fabric groups can be investigated based on a comparison with the geological background of the Baetican region, as well as on the integration of the archaeological evidence to the obtained analytical results.

The fabric group PF 1 is well represented in this study. The typological evidence and the macroscopic characteristics of the samples, that are comparable to those found in some Late Roman workshops of the Guadalquivir/Genil area (*e.g.* Berni, 1998; Remolà, 2000; Romo and Vargas, 2001; Berni and Moros, 2012b), suggest this latter as an initial provenance hypothesis. The petrographic composition of the fabrics is, in fact, compatible with this hypothesis (see Fantuzzi *et al.*, 2015, 2016). The geological background of the Guadalquivir basin and its surroundings present many possible sources of metamorphic and granitic contributions, especially from the Sierra

Morena, while sedimentary calcareous materials are extremely common in the deposits derived from the external zones of the Baetic Cordillera (Subbaetic System) (IGME, 1970, 1980a; Junta de Andalucía, 1998). The existence of Upper Miocene-Pliocene marine sediments in this basin (Solé, 1983; González-Delgado *et al*., 2004) may account for the presence of some marine microfossils in the fabrics (*e.g.* foraminifera, echinoids). A similar petrographic composition, in a coarser fabric, has been documented in some Dressel 20 amphorae produced in the Guadalquivir area during the Early Roman period (Peacock and Williams, 1986).

The two main fabrics in PF 1 (PF 1.1 and 1.2) share the same chemical composition; both comprise samples coming from contexts with a similar chronology (5th century to early 6th century). Their minor petrographic differences are difficult to explain due to the lack of archaeometric studies on the production centres. Possible hypotheses for this variation could be the existence of different workshops or the production at the same workshop but using slightly different raw materials and/or paste recipes.Conversely, the fabric PF 1.3 shows minor differences in both petrographic and chemical composition when compared to the other two fabrics; the only sample in this fabric (ILU003) comes from an early fourth-century context in Mataró. Further studies with an increased sample size will help to clarify if there exist, in fact, compositional differences related to diachronic changes in the Late Roman amphorae from the Guadalquivir/Genil production centres.

The fabric group PF 2, represented by only two samples in this study, presents close similarities in the petrographic components and chemical composition with PF 1. This, in addition to the typological evidence (related to the variant Dressel 23a), suggests the Guadalquivir area as the most plausible provenance hypothesis. The very rare presence of basalt/trachyte in the inclusions (clearly accessory compared to the sedimentary, metamorphic and, to a lesser degree, granitic inclusions) can be fully compatible with the existence of deposits of these rocks in various parts of the Sierra Morena, to the northern part of the Guadalquivir basin between Córdoba and Sevilla (IGME, 1970, 1980a; Junta de Andalucía, 1998). PF 2 shows a higher frequency of quartz and alkali feldspar, and less calcareous inclusions, than PF 1, but both fabric groups share important compositional and technological similarities.

The sample ILU001, that can be possibly (though more questionably) related to type Dressel 23a, comes from the same early fourth-century context as ILU003. It presents a well-differentiated chemical composition and also a particular fabric (PF 3). Its petrographic characteristics are compatible with a hypothetical provenance in the Guadalquivir/Genil area (corresponding to a different production from the others documented in this study), but in any case the compositional particularities of this individual preclude drawing clear conclusions.

Unlike the previous fabrics, the analytical results suggest a different provenance area for the fabric group PF 4, well represented in this study, including samples of Dressel 23d and Almagro 51A-B amphorae mainly. The presence and types of metamorphic and sedimentary rocks in the inclusion composition, as well as the accessory presence of ultrabasic (serpentine) inclusions, points to a provenance in the central-western coastal area of Málaga, close to the outcrops of low-grade metamorphic rocks (phyllite, meta-argillite) and sedimentary rocks (argillite, mudstone, greywacke, conglomerate, limestone) of the Maláguide Complex, and of higher-grade metamorphic rocks (schist, quartzite, gneiss, phyllite, marble, amphibolite, among others) and peridotite from the Alpujárride Complex, in addition to the sedimentary contribution derived from other formations in the area (IGME, 1972a, 1972b, 1980b; Junta de Andalucía, 1998; Serrano and Guerra, 2004) (Figure 12). The Maláguide and Alpujárride complexes are part of the internal zones of the Betic-Rif Arc (or Gibraltar Arc), while the external zones comprise —in the regional geology of Málaga— sedimentary deposits (calcareous mainly) from the Triassic (Trias of Antequera) and Jurassic/Cretacic (Subbaetic and Penibaetic systems); other sedimentary contributions in the area are related to the Paleogene to Miocene units of Campo de Gibraltar, and the post-orogenic formations (Miocene, Pliocene and Quaternary). This provenance hypothesis for PF 4 is fully compatible with the archaeological and typological evidence, since the production of both Dressel 23 and Almagro 51A-B amphorae has been attested for some workshops in the Málaga coast, including those located at the central-western part of this area, *e.g.* Huerta del Rincón (Torremolinos) or Calle Almansa-Cerrojo (Málaga). The sediments close to the mouth of the Guadalhorce river may contain materials derived from the mentioned geological sources (Figure 12); this would support a provenance in some of these workshops, or in any other possible workshop located in the same area.

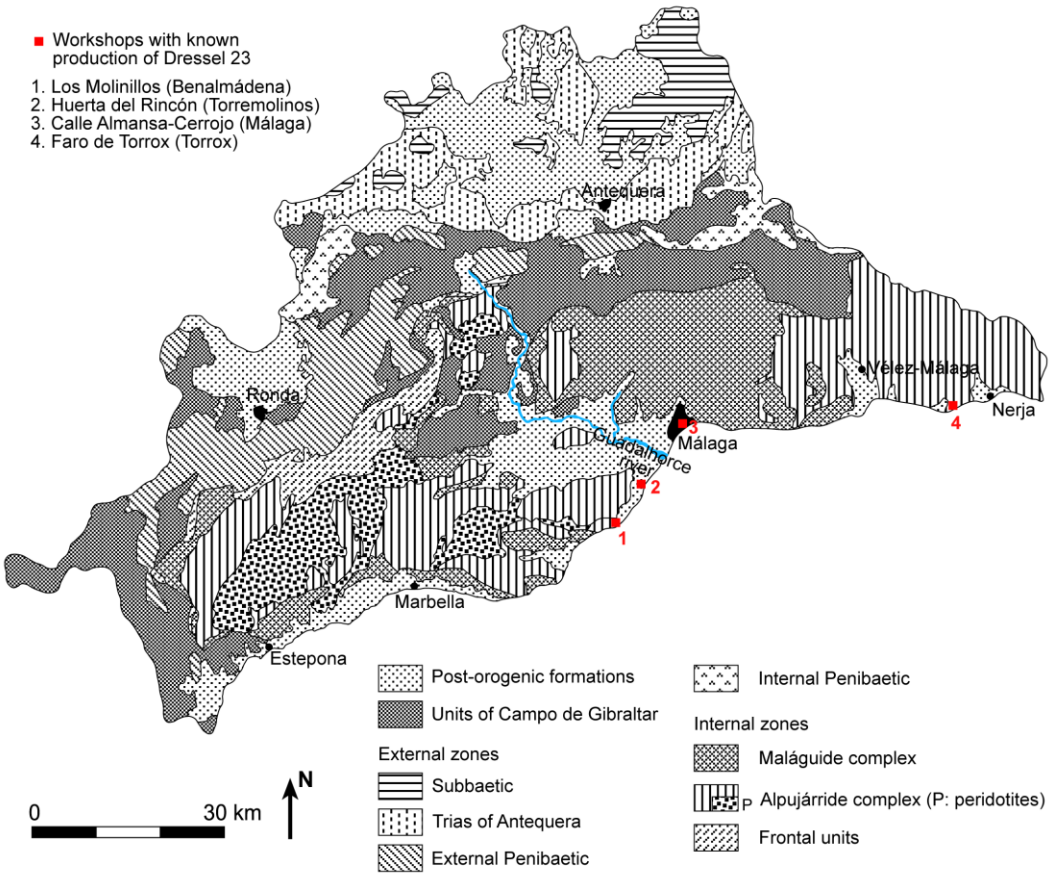

Figure 12. Geological map of the province of Málaga, with an indication of the workshops where the production of Dressel 23 amphorae has been attested so far (modified from Serrano and Guerra 2004, and Corrales et al. 2011)

The production of the amphora type Almagro 51A-B, traditionally associated with the transport of fish sauce (*salsamenta*), is well documented in different zones of the Baetican and Lusitanian coast, however the variant Keay 19A-B is considered to be a Baetican product (Remolà, 2000; Bernal, 2001). This is a typical amphora from the southern Hispanic coast, without any archaeological evidence of its production in the Guadalquivir valley. A certain variety of fabrics exists for this type of amphora, but for the present study we have selected only samples with macroscopic fabric similarities to the Dressel 23d samples. The analytical results in this paper prove that there is, in fact, a close relationship between these amphorae, with samples of both types sharing the same chemical-petrographic compositions. In summary, the integration of the archaeometric and the archaeological data clearly suggests a coastal Baetican provenance for PF 4, in particular in the central-western Málaga area.

The majority of the samples in PF 4 belong to the same fabric (PF 4.1), with some variations in colour and texture that can mainly relate to firing temperatures, as shown by the analytical results. Other fabrics, poorly represented in this study (PF 4.2 to 4.4), must be associated with the same general provenance area, though an adequate interpretation of this diversity (different workshops? different paste recipes in a same workshop?) is not possible at this time due to the actual state of research in the production centres. All these fabrics include samples from fifth- and sixth-century contexts, except PF 4.3 with only one sample (ABA002), an earlier chronology (4th century) and a different typology (Table 1). These differences should be borne in mind but, in any case, further studies are needed to demonstrate if this fabric is also present in later chronologies and/or in other amphora types.

Similar conclusions than for PF 4 can be drawn concerning the provenance of the fabric group PF 5, poorly represented in this study but including samples (MC0359, MC0387) that belong, again, to the types Dressel 23d and Almagro 51A-B. The petrographic composition shows a resemblance to PF 4, in particular the types of metamorphic rock fragments that compose the temper, that seem to suggest a close provenance area; also the broad chemical similarities between these fabric groups would support

this hypothesis. In this case, unlike PF 4, the absence of ultrabasic inclusions does not restrict the provenance hypothesis to the central-western part of the Málaga coast, since it could be also compatible with the eastern part, but the general petrographic composition still suggests the former as a possible provenance area.

A different composition is seen in the fabric PF 6, represented by one sample (MC0356) of the type Dressel 23d. The chemical similarities with PF 5 (Figure 6-7; Table 3) suggest a certain relationship between these fabrics, but the petrographic particularities indicate a different provenance. It is, again, a clearly metamorphic fabric, but in this case contains a higher frequency of metamorphic minerals such as garnet and staurolite. These components are frequent in deposits derived from the Alpujárride complex (as well as in the Nevado-Filábride complex in southeastern Spain, farther from the production area of Dressel 23 amphorae) and would more likely suggest a provenance in the eastern coast of Málaga or the coast of Granada (IGME, 1980b; Junta de Andalucía, 1998). Production of Dressel 23 has been documented in the former (*e.g.* Faro de Torrox, see Rodríguez, 1997) and, less likely, in the latter (Los Barreros, see Bernal and Navas, 1998). Further studies from these zones will help to clarify the precise provenance of this fabric within the Baetican coastal area.

5. CONCLUSIONS

The archaeometric study of Dressel 23 amphorae from consumption centres reveals a variety of chemical-petrographic compositions that can be related to more than one provenance area. On the one hand, there are fabric groups associated with a provenance in the Guadalquivir/Genil area that include all the analysed samples of variants Dressel 23a and 23c (PF 1 and 2, possibly also PF 3). On the other hand, all the samples belonging to the variant Dressel 23d and 23d similis, as well as to the type Almagro 51A-B/Keay 19A-B, are included in the fabric groups PF 4, 5 and 6, with a provenance in the Baetican coast and, in particular, in the coast of Málaga; PF 4 is the most represented of the three, and its compositional particularities indicate a production in the central-western coast of Málaga. The variant Dressel 23d has been defined by archaeologists on the basis not only of its morphological characteristics but also of its fabric particularities to the naked eye (Berni, 1998; Remolà, 2000; Berni and Moros, 2012b). The present study indicates, on analytical grounds, that this variant of Dressel 23 must be related to a provenance in the Baetican coast rather than in the Guadalquivir area. In any case, a certain variety of petrographic fabrics exist, both for the Dressel 23a and the Dressel 23d variants, thus indicating the arrival of amphorae from different workshops to the consumption centres. For some of these fabrics (PF 1.1, 1.2, 4.1), a certain macroscopic variability (*e.g.* colour, texture) can be related to technical considerations, such as the firing temperatures, rather than to differences in the used clayey raw materials.

Even if the Guadalquivir/Genil is normally accepted as the main production and export area of Dressel 23 amphorae, the possibility of an origin in Málaga for Dressel 23d should lead to some caution when interpreting the archaeological findings, especially if we bear in mind its relatively high frequency in some consumption centres, *e.g.* it is as frequent as Dressel 23a in the contexts of *Tarraco*/Tarragona, and even more frequent in some large contexts such as the rubbish dump of Vila-roma (Remolà, 2000). This could have strong implications on the interpretation of the relative weight that each production area had on the Late Roman commercial dynamics.

Further implications may derive from the possible content of these amphorae. For the Dressel 23 from the Guadalquivir/Genil area, the hypothesis of oil transport is largely accepted due to the existing strong evidence base (see Bernal, 2001). With regard to the Dressel 23 from Málaga, its production has been documented in workshops that were mainly producing salted-fish amphorae (Almagro 51A-B, Almagro 51C, among others), although the hypothesis of oil transport has been based traditionally on indirect evidence, including its morphological relationship to amphorae from the Guadalquivir/Genil area as well as archaeological evidence of oil production in the Málaga coastal territory (see Bernal, 1997; Padilla, 2001). A recent organic residue analysis by Pecci and Cau (2014) provided direct evidence of the presence of vegetable oil in Dressel 23d (MC0356) and Dressel 23d similis (MC0355) amphorae. If this hypothesis is supported by further studies, the role of the Málaga region as an important export area of oil (in addition to the well-known export of *salsamenta*) during the Late Roman period should start to be taken into consideration in archaeological studies.

ACKNOWLEDGEMENTS

This work was performed in the framework of the project Late Roman Pottery in the Western Mediterranean: exploring regional and global trade networks through experimental sciences (LRPWESTMED) (ref. HAR2013-45874-P), funded by the Plan Nacional de I+D+I Ministerio de Economía y Competitividad,

Secretaría de Estado de Investigación, Desarrollo e Innovación, with contributions from FEDER funds (PI: Miguel Ángel Cau Ontiveros). This is part of the activities of the Equip de Recerca Arqueològica i Arqueomètrica de la Universitat de Barcelona (ERAAUB), Consolidated Group (2014 SGR 845), thanks to the support of the Comissionat per a Universitats i Recerca del DIUE de la Generalitat de Catalunya.

XRF, XRD and SEM-EDS analyses were undertaken at the Centres Científics i Tecnològics of the University of Barcelona. We are grateful to Josep Maria Macias (ICAC), Imma Teixell and Andreu Muñoz for the provision of the samples from the Cathedral of Tarragona; to J. M. Macias also for the samples from the Amphitheatre of Tarragona; to Josep Anton Remolà (Museu Nacional Arqueològic de Tarragona) for the samples from Vila-Roma; to the Museu de Mataró for the samples from Mataró; and to X. Aquilué and the rest of colleagues from the Museu d'Arqueologia de Catalunya-Empúries (in particular to P. Castanyer, J. Tremoleda and M. Santos) for the samples from Sant Martí d'Empúries. We are grateful to Kik Williams for the English revision and to two anonymous referees for their helpful comments.

REFERENCES

Aitchison, J. (1986) *The statistical analysis of compositional data*. Chapman and Hall, London.

Aitchison, J. (1992) On criteria for Measures of Compositional Difference. *Mathematical Geology*, 24, 365-379.

Alarção, A. and Mayet, F. (eds.) (1990) *As Ânforas lusitanas: Tipologia, produção, comércio. Actas das jornadas de estudo realizadas em Conimbriga em 13 et 14 de Outobro 1988*. Boccard, Paris.

Aquilué, X. and Burés, L. (1999) La ciutat en l´antiguitat tardana: fase V. In Aquilué, X. (ed.), *Intervencions arqueològiques a Sant Martí d´Empúries (1994-1996). De l´assentament precolonial a l´Empúries actual*, Museu d'Arqueologia de Catalunya, Empúries, pp. 389-422.

Baldomero, A., Corrales, P., Escalante, M.M., Serrano, E. and Suárez, J. (1997) El alfar romano de la Huerta del Rincón: síntesis tipológica y momentos de producción. In *Figlinae Malacitanae: la producción de cerámica romana en los territorios malacitanos*, Área de Arqueología de la Universidad de Málaga, Málaga, pp. 147-176.

Bernal, D. (1997) Las producciones ánforicas del Bajo Imperio y de la Antigüedad Tardía en Málaga. Estado actual de la investigación e hipótesis de trabajo. In *Figlinae Malacitanae: la producción de cerámica romana en los territorios malacitanos*, Área de Arqueología de la Universidad de Málaga, Málaga, pp. 233-260.

Bernal, D. (2001) La producción de ánforas en la Bética en el s. III y durante el bajo imperio romano. In *Congreso Internacional Ex Baetica Amphorae. Conservas, aceite y vino de la Bética en el Imperio Romano (Écija, Sevilla, 1998)*, Actas Gráficas Sol, Écija, pp. 239-372.

Bernal, D. and Lagóstena, L. (Eds.) (2004) *Figlinae Baeticae: talleres alfareros y producciones cerámicas en la Bética romana (ss. II a.C.-VII d.C.). Actas del Congreso Internacional, Cádiz, 12-14 de noviembre de 2003*. BAR International Series 1266, Archaeopress, Oxford.

Bernal, D. and Navas, J. (1998) La producción alfarera en la costa granadina en época romana. In Bernal, D. (ed.), *Los Matagallares (Salobreña, Granada). Un centro romano de producción alfarera en el siglo III d.C. Primeros resultados de las excavaciones arqueológicas de las campañas de 1995 y 1996*, Ayuntamiento de Salobreña, Salobreña, pp. 63-100.

Berni, P. (1998) *Las ánforas de aceite de la Bética y su presencia en la Cataluña romana*. Publicacions Universitat de Barcelona, Barcelona.

Berni, P. and Moros, J. (2012a) Los sellos in planta pedis de las ánforas olearias béticas Dressel 23 (primera mitad siglo V d.C.). *Archivo Español de Arqueología*, 85, 193-219.

Berni, P. and Moros, J. (2012b) Dressel 23 (Valle del Guadalquivir). In *Amphorae ex Hispania. Paisajes de producción y de consumo*. http://amphorae.icac.cat/tipol/view/2 (accessed june 2016).

Buxeda, J. (1999). Alteration and contamination of archaeological ceramics: the perturbation problem. *Journal of Archaeological Science*, 26, 295–313.

Buxeda, J. and Cau, M.A. (2004) Annex I. Caracterització arqueomètrica de les produccions tardanes d'Iluro. In Cela, X. and Revilla, V. (eds.), *La transició del municipium d'Iluro a Alarona (Mataró). Cultura material i transformacions d'un espia urbà entre els segles V i VII dC*, Laietània 15, Museu Municipal de Mataró, Mataró, pp. 449-498.

Buxeda, J., Cau, M.A., Loschi, A.G. and Medici, A. (1998) Caracterización arqueométrica de las ánforas tardías de la cisterna de Sa Mesquida (Santa Ponça, Calvià, Mallorca). Resultados preliminares. In *El vi a l'Antiguitat. Economia, producció i comerç al Mediterrani occidental. Actes del 2on Col·loqui Internac-*

ional d'Arqueologia Romana (Badalona, 6-9 de maig de 1998), Museu de Badalona, Badalona, pp. 530-542.

Buxeda, J. and Kilikoglou, V. (2003) Total variation as a measure of variability in chemical data sets. In Van Zelst, L. (ed.), *Patterns and process: a Festschrift in honor of Dr. Edward V. Sayre*, Smithsonian Center for Materials Research and Education, Washington DC, pp. 185–198.

Buxeda, J., Mommsen, H. and Tsolakidou, A. (2002) Alterations of Na, K and Rb concentrations in Mycenaean pottery and a proposed explanation using X-ray diffraction. *Archaeometry*, 44, 187-198.

Cela, X. and Revilla, V. (2004) *La transició del municipium d'Iluro a Alarona (Mataró). Cultura material i transformacions d'un espia urbà entre els segles V i VII dC*. Laietània 15, Museu Municipal de Mataró, Mataró.

Cerdà, J.A., García, J., Martí, C., Pera, J., Pujol, J. and Revilla, V. (1997) *El cardo maximus de la ciutat romana d'Iluro (Hispania Tarraconesis)*. Laietània 10, Museu Municipal de Mataró, Mataró.

Chic, G. and García, E. (2004) Alfares y producciones cerámicas en la provincia de Sevilla. Balance y perspectivas. In Lagóstena, L. and Bernal, D. (eds.), *Figlinae Baeticae: talleres alfareros y producciones cerámicas en la Bética romana (ss. II a.C.-VII d.C.). Actas del Congreso Internacional, Cádiz, 12-14 de noviembre de 2003*, BAR International Series 1266, Archaeopress, Oxford, pp. 279-348.

Ciurana, J., Macias, J.M., Muñoz, A. and Teixell, I. (2011) *Memòria de la intervenció arqueològica a les fosses de l'amfiteatre romà de Tarragona*. Unpublished report, Departament de Cultura de la Generalitat de Catalunya, Tarragona.

Ciurana, J., Macias, J.M., Muñoz, A., Teixell, I. and Toldrà, J.M. (2013) *Amphitheatrvm, memoria martyrvm et eclesiae. Les intervencions arqueològiques a l'amfiteatre de Tarragona (2009-2012)*. Ajuntament de Tarragona - Institut Català d'Arqueologia Clàssic - Mvsevm Biblicvm Tarraconense - Associació Cultural Sant Fructuós, Tarragona.

Corrales, P., Compaña, J.M., Corrales, M. and Suárez, J. (2011) Salsamenta malacitano. Avances de un proyecto de investigación. *Itálica, Revista de Arqueología Clásica de Andalucía*, 1, 29-49.

Cultrone, G., Rodriguez-Navarro, C., Sebastian, E., Cazalla, O. and De la Torre, M.J. (2001) Carbonate and silicate phase reactions during ceramic firing. *European Journal of Mineralogy*, 13, 621-634.

Fabião, C. (2008) Las ánforas de Lusitania. In Bernal, D. and Ribera, A. (eds.), *Cerámicas hispanorromanas: un estado de la cuestión*, Servicio de Publicaciones de la Universidad de Cádiz, Cádiz, pp. 725-745.

Fantuzzi, L., Cau, M.A. and Macias, J.M. (2015) Amphorae from the Late Antique city of Tarraco-Tarracona (Catalonia, Spain): archaeometric characterization. *Periodico di Mineralogia*, 84, 1, 169-212.

Fantuzzi, L., Cau, M.A. and Aquilué, X. (2016) Archaeometric characterization of amphorae from the Late Antique city of Emporiae (Catalonia, Spain). *Archaeometry*, 58, Supplement S1, 1–22.

García Vargas, E. and Bernal, D. (2008) Ánforas de la Bética. In Bernal, D. and Ribera, A. (eds.), *Cerámicas hispanorromanas: un estado de la cuestión*, Servicio de Publicaciones de la Universidad de Cádiz, Cádiz, pp. 661-687.

González-Delgado, J.A., Civis, J., Dabrio, C.J., Goy J.L., Ledesma, S., Pais, J., Sierro, F.J. and Zazo, C. (2004) Cuenca del Guadalquivir. In Vera, J.A. (ed.), *Geología de España*, Sociedad Geológica de España – Instituto Geológico y Minero de España, Madrid, pp. 543-550.

Hurlbut, Jr., C.S. and Klein, C. (1993) *Manual of mineralogy*. Wiley, New York.

IGME [Instituto Geológico y Minero de España] (1970) *Mapa Geológico de España, E. 1:200.000, Sevilla, Hoja 75*. Departamento de Publicaciones del Instituto Geológico y Minero de España, Madrid.

IGME [Instituto Geológico y Minero de España] (1972a) *Mapa Geológico de España, E. 1:200.000, Algeciras, Hoja 87*. Departamento de Publicaciones del Instituto Geológico y Minero de España, Madrid.

IGME [Instituto Geológico y Minero de España] (1972b) *Mapa Geológico de España, E. 1:200.000, Morón de la Frontera, Hoja 82*. Departamento de Publicaciones del Instituto Geológico y Minero de España, Madrid.

IGME [Instituto Geológico y Minero de España] (1980a) *Mapa Geológico de España, E. 1:200.000, Córdoba, Hoja 76*. Departamento de Publicaciones del Instituto Geológico y Minero de España, Madrid.

IGME [Instituto Geológico y Minero de España] (1980b) *Mapa Geológico de España, E. 1:200.000, Granada-Málaga, Hoja 83*. Departamento de Publicaciones del Instituto Geológico y Minero de España, Madrid.

Járrega, R. (1993) *Poblamiento y economia en la costa Este de la Tarraconense en època tardorromana (siglos IV-VI)*. Unpublished doctoral dissertation, Universitat Autònoma de Barcelona, Barcelona.

Járrega, R. (2013) Las últimas importaciones romanas de cerámica en el Este de Hispania Tarraconensis: una aproximación. *Spal*, 22, 143-172.

Junta de Andalucía (1998) *Mapa Geológico-Minero de Andalucía. Escala 1:400.000 (3ª Versión)*. Dirección General de Industria, Energía y Minas, Sevilla.

Keay, S.J. (1984) *Late Roman Amphorae in the Western Mediterranean. A tipology and economic study: the Catalan evidence*. British Archaeological Reports, Oxford.

Kretz, R. (1983) Symbols for rock-forming minerals. *American Mineralogist*, 68, 277-279.

Macias, J.M., Menchon, J.J., Muñoz, A. and Teixell, I. (2008) Contextos cerámicos derivados de la transformación cristiana de la acrópolis de Tarragona (s. V/VI d.C.). In Rivet, L. (ed.), *SFECAG - Actes du congrès de l'Escala-Empúries, 1er-4 mai 2008*, Société Française d'Étude de la Céramique Antique en Gaule, Marseille, pp. 287-293.

Maggetti, M. (1982) Phase analysis and its significance for technology and origin. In Olin, J.S. and Franklin, A.D. (eds.), *Archaeological Ceramics*, Smithsonian Institution Press, Washington DC, pp. 121-133.

Maggetti, M., Neururer, C. and Ramseyer, D. (2011) Temperature evolution inside a pot during experimental surface (bonfire) firing. *Applied Clay Science*, 53, 500-508.

Maniatis, Y. and Tite, M.S. (1981) Technological examination of Neolithic-Bronze age pottery from central and southeast Europe and from the Near East. *Journal of Archaeological Science*, 8, 59-76.

Mayet, F., Schmitt, A. and Tavares, C. (1996) *Les amphores du Sado (Portugal)*. Diffusion E. de Boccard, Paris.

Orfila, M. (1989) Cerámicas de la primera mitad del siglo V d.C. procedentes de la cisterna de Sa Mesquida (Santa Ponça, Mallorca). *L'Africa Romana*, 6, 513-533.

Overstreet, W.C. (1967) *The geologic occurrence of monazite*. Geological Survey Professional Paper 530, United States Government Printing Office, Washington DC.

Padilla, A. (2001) Comercio y comerciantes en el mundo tardorromano en Málaga. In *Comercio y comerciantes en la Historia Antigua de Málaga (Siglo VIII a.C. – año 711 d.C.). II Congreso de Historia Antigua de Málaga*, Servicio de Publicaciones, Centro de Ediciones de la Diputación de Málaga, Málaga, pp. 385-417.

Peacock, D.P.S. and Williams, D.F. (1986) *Amphorae and the Roman economy, an introductory guide*. Longman, London/New York.

Pecci, A. and Cau, M.A. (2014) Residue analysis of Late Roman cooking pots and amphorae from Sa Mesquida (Mallorca, Balearic Islands). In Poulou-Papadimitriou, N., Nodarou, E. and Kilikoglou, V. (eds.), *LRCW 4. Late Roman Coarse Wares, Cooking Wares and Amphorae in the Mediterranean: Archaeology and archaeometry. The Mediterranean: a market without frontiers*, BAR International Series 2616, Archaeopress, Oxford, pp. 833-841.

Quinn, P.S. (2013) *Ceramic Petrography. The interpretation of archeological pottery and related artefacts in thin section*. Archaeopress, Oxford.

Remesal, J. (1983) Transformaciones en la exportación del aceite bético a mediados del siglo III d.C. In *Producción y comercio del aceite en la antigüedad, II Congreso Internacional (Sevilla, 1982)*, Universidad Complutense, Madrid, pp. 131-152.

Remesal, J. (1991) El aceite bético durante el Bajo Imperio. In González, A., Fernández, F.J. and Remesal, J. (eds.), *Arte, sociedad, economía y religión durante el Bajo Imperio y la Antigüedad Tardía*, Universidad de Murcia, Murcia, pp. 355-361.

Remesal, J. (2004) Alfares y producciones cerámicas en la provincia de Córdoba. Balance y perspectivas. In Lagóstena, L. and Bernal, D. (eds.), *Figlinae Baeticae: talleres alfareros y producciones cerámicas en la Bética romana (ss. II a.C.-VII d.C.). Actas del Congreso Internacional, Cádiz, 12-14 de noviembre de 2003*, BAR International Series 1266, Archaeopress, Oxford, pp. 349-361.

Remolà, J.A. (2000) *Las ánforas tardo-antiguas en Tarraco (Hispania Tarraconensis)*. Publicacions Universitat de Barcelona, Barcelona.

Reynolds, P. (2010) *Hispania and the Roman Mediterranean, AD 100-700. Ceramics and Trade*. Duckworth, London.

Roberts, J.P. (1963) Determination of the firing temperature of ancient ceramics by measurement of thermal expansion. *Archaeometry*, 6, 21-25.

Rodríguez, P. (1997) Los hornos cerámicos del Faro de Torrox (Málaga). In *Figlinae Malacitanae: la producción de cerámica romana en los territorios malacitanos*, Área de Arqueología de la Universidad de Málaga, Málaga, pp. 271-303.

Romo, A. and Vargas, J.M. (2001) Azanaque. Evidencias arqueológicas de un centro de producción anfórica. In *Congreso Internacional Ex Baetica Amphorae. Conservas, aceite y vino de la Bética en el Imperio Romano (Écija, Sevilla, 1998), Actas*, Gráficas Sol, Écija, pp. 405-417.

Schwedt, A., Mommsen, H., Zacharias, N. and Buxeda, J. (2006) Analcime crystallization and compositional profiles — comparing approaches to detect post-depositional alterations in archaeological pottery. *Archaeometry*, 48, 2, 237-251.

Serrano, E. (2004) Alfares y producciones cerámicas en la provincia de Málaga: balance y perspectivas. In Lagóstena, L. and Bernal, D. (eds.), *Figlinae Baeticae: talleres alfareros y producciones cerámicas en la Bética romana (ss. II a.C.-VII d.C.). Actas del Congreso Internacional, Cádiz, 12-14 de noviembre de 2003*, BAR International Series 1266, Archaeopress, Oxford, pp. 161-194.

Serrano, F. and Guerra, A. (2004) *Geología regional. El territorio de la provincia de Málaga en el ámbito de la cordillera Bética*. Universidad de Málaga, Málaga.

Solé, L. (1983) Morfología General de la Península Ibérica. In Comba, J.A. (ed.), *Libro jubilar J. M. Ríos. Geología de España, Tomo II*, Instituto Geológico y Minero de España, Madrid, pp. 589-605.

TED'A [Taller-Escola d'Arqueologia] (1989) *Un abocador del segle V d.C. en el fòrum provincial de Tàrraco*. Taller Escola d'Arqueologia, Tarragona.

Teixell, I., Macias, J.M. and Menchon, J.J. (2005) *Memòria de les intervencions arqueològiques a la Catedral de Tarragona - Museu Diocesà*. Unpublished report, Servei d'Arqueologia i Paleontologia de la Generalitat de Catalunya, Barcelona.

Tite, M.S., Freestone, I.C., Meeks, N.D. and Bimson, M. (1982) The use of scanning electron microscopy in the technological examination of ancient ceramics. In Olin, J.S. and Franklin, A.D. (eds.), *Archaeological Ceramics*, Smithsonian Institution Press, Washington DC, pp. 109-120.

Whitbread, I.K. (1989) A proposal for the systematic description of thin sections towards the study of ancient ceramic technology. In Maniatis, Y. (ed.), *Archaeometry: proceedings of the 25th international symposium*, Elsevier, Amsterdam, pp. 127-138.

Whitbread, I.K. (1995) Appendix 3. The collection, processing and interpretation of petrographic data. In *Greek transport amphorae: a petrological and archaeological study*, British School at Athens, Athens, pp. 365-396.